

# A positive feedback between p53 and *miR-34* miRNAs mediates tumor suppression

Nobuhiro Okada,<sup>1</sup> Chao-Po Lin,<sup>1</sup> Marcelo C. Ribeiro,<sup>1</sup> Anne Biton,<sup>2</sup> Gregory Lai,<sup>1</sup> Xingyue He,<sup>3</sup> Pengcheng Bu,<sup>1</sup> Hannes Vogel,<sup>4</sup> David M. Jablons,<sup>5</sup> Andreas C. Keller,<sup>6,7</sup> J. Erby Wilkinson,<sup>8</sup> Biao He,<sup>5</sup> Terry P. Speed,<sup>2</sup> and Lin He<sup>1,9</sup>

<sup>1</sup>Molecular and Cell Biology Department, University of California at Berkeley, Berkeley, California 94705, USA; <sup>2</sup>Department of Statistics, University of California at Berkeley, Berkeley, California 94705, USA; <sup>3</sup>Takeda Oncology Company, Cambridge, Massachusetts 02139, USA; <sup>4</sup>Department of Pathology, Stanford University School of Medicine, Stanford, California 94305, USA; <sup>5</sup>Thoracic Oncology Program, Department of Surgery, University of California at San Francisco, San Francisco, California 94115, USA; <sup>6</sup>Department of Clinical Bioinformatics, Saarland University, University Hospital, 66041 Saarbrücken, Germany; <sup>7</sup>Technology Innovation, Siemens Healthcare, 91052 Erlangen, Germany; <sup>8</sup>Department of Pathology, University of Michigan, Ann Arbor, Michigan 48109, USA

As bona fide p53 transcriptional targets, *miR-34* microRNAs (miRNAs) exhibit frequent alterations in many human tumor types and elicit multiple p53 downstream effects upon overexpression. Unexpectedly, *miR-34* deletion alone fails to impair multiple p53-mediated tumor suppressor effects in mice, possibly due to the considerable redundancy in the p53 pathway. Here, we demonstrate that *miR-34a* represses *HDM4*, a potent negative regulator of p53, creating a positive feedback loop acting on p53. In a *Kras*-induced mouse lung cancer model, *miR-34a* deficiency alone does not exhibit a strong oncogenic effect. However, *miR-34a* deficiency strongly promotes tumorigenesis when p53 is haploinsufficient, suggesting that the defective p53–*miR-34* feedback loop can enhance oncogenesis in a specific context. The importance of the p53/*miR-34*/*HDM4* feedback loop is further confirmed by an inverse correlation between *miR-34* and full-length *HDM4* in human lung adenocarcinomas. In addition, human lung adenocarcinomas generate an elevated level of a short *HDM4* isoform through alternative polyadenylation. This short *HDM4* isoform lacks *miR-34*-binding sites in the 3' untranslated region (UTR), thereby evading *miR-34* regulation to disable the p53–*miR-34* positive feedback. Taken together, our results elucidated the intricate cross-talk between p53 and *miR-34* miRNAs and revealed an important tumor suppressor effect generated by this positive feedback loop.

[Keywords: *miR-34*; microRNAs; p53; Mdm4; *HDM4*]

Supplemental material is available for this article.

Received October 25, 2013; revised version accepted January 15, 2014.

p53, the “guardian of the genome,” functions at the center of a complex molecular network to mediate tumor suppression (Riley et al. 2008; Vousden and Prives 2009; Lane and Levine 2010). In response to various oncogene and cellular stresses, p53 activates or represses a large number of downstream targets in a context- and stimulus-dependent manner, promoting multiple cellular processes to collectively repress tumor formation (Riley et al. 2008). In addition to the numerous protein-coding p53 targets, noncoding RNAs—in particular, microRNAs (miRNAs)—are increasingly recognized as essential components of the p53 pathway to mediate post-transcriptional gene repression downstream from p53 (Hermeking 2007; Lin et al. 2012).

miRNAs are a class of small, regulatory noncoding RNAs that mediate post-transcriptional gene silencing of

specific mRNAs (Ambros 2004; Zamore and Haley 2005; Filipowicz et al. 2008; Bartel 2009). Among the best-studied p53-regulated miRNAs are *miR-34* miRNAs, including *miR-34a*, *miR-34b*, and *miR-34c*, which are encoded at two distinct loci: *mir-34a* and *mir-34b/34c* (Chang et al. 2007; He et al. 2007; Raver-Shapira et al. 2007; Tarasov et al. 2007). Acute *miR-34* overexpression elicits various p53 downstream effects in a context-dependent manner, including cell cycle arrest, apoptosis, senescence, and suppression of the epithelial–mesenchymal transition (EMT) (Chang et al. 2007; He et al. 2007; Raver-Shapira et al. 2007; Kim et al. 2011). Such *miR-34* effects are mediated at least in part by post-transcriptional repression of targets, including cyclin D1, cyclin E2, Cdk4,

<sup>9</sup>Corresponding author  
E-mail [lhe@berkeley.edu](mailto:lhe@berkeley.edu)

Article published online ahead of print. Article and publication date are online at <http://www.genesdev.org/cgi/doi/10.1101/gad.233585.113>.

© 2014 Okada et al. This article is distributed exclusively by Cold Spring Harbor Laboratory Press for the first six months after the full-issue publication date (see <http://genesdev.cshlp.org/site/misc/terms.xhtml>). After six months, it is available under a Creative Commons License [Attribution-NonCommercial 3.0 Unported], as described at <http://creativecommons.org/licenses/by-nc/3.0/>.

c-Met, c-Myc, Bcl2, Snail1, and Sirt1, which collectively promote multiple oncogenic processes (Hermeking 2009). More importantly, acute *miR-34* expression also leads to tumor repression in vivo in both a genetically engineered lung adenocarcinoma model and multiple xenograft models (Wiggins et al. 2010; Kasinski and Slack 2012). Consistently, a low-level *miR-34* expression has been detected in a variety of human cancer types due to aberrant transcriptional regulation, genomic deletions, and promoter hypermethylation (Kaghad et al. 1997; Lodygin et al. 2008; Hermeking 2009; Wang et al. 2011b; Tanaka et al. 2012). These observations imply the functional significance of *miR-34* deficiency in tumorigenesis and suggest that *miR-34* miRNAs could act as important components of the tumor suppressor network.

Unexpectedly, the initial phenotypic characterization of *miR-34* knockout mice has yielded a confusing picture. *miR-34*-deficient mouse embryonic fibroblasts (MEFs) exhibited no defects in p53-dependent cell cycle arrest, apoptosis, or replicative senescence (Choi et al. 2011; Concepcion et al. 2012). In addition, the *mir-34a*<sup>-/-</sup>; *mir-34b/34c*<sup>-/-</sup> mouse showed no increase in p53-dependent spontaneous tumorigenesis, irradiation-induced lymphomagenesis, or oncogenic cooperation in the *Eμ-myc* B-cell lymphoma model (Concepcion et al. 2012). In these contexts, it is conceivable that the redundant pathways downstream from p53 could compensate for *miR-34* loss in vivo. Nevertheless, deficiency of *mir-34a* or *mir-34b/34c* partially phenocopies p53 deficiency in promoting somatic reprogramming (Choi et al. 2011), implicating that *miR-34* miRNAs can mediate the p53 downstream effects in a context-dependent manner (Jain and Barton 2012). Due to the redundant nature of the p53 pathway, we hypothesize that the function of the p53–*miR-34* axis in tumor suppression could be best revealed in systems where the robustness of the p53 response is compromised.

In this study, we demonstrated a positive feedback loop between p53 and *miR-34a* that is at least in part due to the *miR-34a*-mediated repression of a negative p53 regulator, Mdm4. Using a *Kras*-induced mouse lung adenocarcinoma model, we demonstrated the functional importance of this p53–*miR-34a* positive feedback in tumor suppression. Given the redundancy of the p53 network, the p53–*miR-34* positive feedback confers an important tumor suppressor effect that is only evident when p53 is haploinsufficient in vivo. Consistently, human lung adenocarcinomas, when compared with normal lung tissues, not only exhibit an inverse correlation between *miR-34* and full-length *HDM4* but also have an elevated level of a shorter *HDM4* isoform that evades *miR-34*-dependent regulation. Altogether, our studies elucidate an intricate cross-talk between p53 and *miR-34* miRNAs and reveal the oncogenic consequences when this feedback loop is disrupted in vivo.

## Results

### *miR-34a* deficiency promotes *Kras*<sup>G12D</sup>-induced lung adenocarcinomas when p53 is haploinsufficient

Emerging evidence implicates the p53-regulated *miR-34* miRNAs as integral components of the tumor suppressor

pathway in the development of lung adenocarcinomas (Wiggins et al. 2010; Kasinski and Slack 2012). *miR-34* loci were frequently hypermethylated and down-regulated in human non-small-cell lung cancers (NSCLCs) (Lodygin et al. 2008; Wang et al. 2011b; Tanaka et al. 2012). Similarly, the expression of *miR-34* was readily detected in both neonatal and adult mouse lungs but was significantly decreased in the terminal lung adenocarcinomas induced by activating *Kras* mutation (*Kras*<sup>G12D</sup>) and p53 deletion (Fig. 1A,B; Supplemental Fig. S1A,B). Consistently, enforced exogenous *miR-34* expression prevented the initiation and progression of lung cancer development in mice in both a xenograft model and a genetically engineered lung adenocarcinoma model induced by *Kras*<sup>G12D</sup> and a dominant-negative p53<sup>R172H</sup> mutation (Wiggins et al. 2010; Kasinski and Slack 2012). These findings led us to hypothesize that *miR-34* miRNAs, as integral components of the p53 pathway, could play an important role in suppressing lung cancer development.

Activating mutations in *Kras*, which occur in ~30% of human NSCLCs, act as a strong initiation lesion to promote the development of lung adenomas and adenocarcinomas in mice (Slebos et al. 1990; Rodenhuis and Slebos 1992). A genetically engineered *Kras*<sup>LSL-G12D</sup> mouse strain has been widely employed to study the development of lung cancer (Jackson et al. 2001; Winslow et al. 2011). In this mouse model, the expression of the oncogenic *Kras*<sup>G12D</sup> allele from its endogenous promoter can be specifically induced in lung by Adeno-Cre (AdCre) virus-mediated removal of a transcription termination element flanked with LoxP sites (designated as LSL cassette) (Jackson et al. 2001).

Aberrant Ras signaling, triggered by either Hras overexpression or the activating *Kras*<sup>G12D</sup> mutation, induces *miR-34* expression in a p53-dependent manner (Supplemental Fig. S1C; He et al. 2007). Using the *Kras*<sup>LSL-G12D</sup> lung cancer model, we investigated the tumor suppressor functions of *miR-34a* in vivo. The loss of *miR-34a* alone exhibited no significant oncogenic cooperation with *Kras*<sup>G12D</sup> in the lung (Fig. 1C; Supplemental Fig. S1D). This finding is similar to a number of canonical p53 targets whose knockout in mice fail to promote tumorigenesis in vivo to the extent of p53 deficiency (Martín-Caballero et al. 2001; Choudhury et al. 2007; Michalak et al. 2008). These findings imply the complex nature of functional redundancy downstream from p53 and suggest that the in vivo effects of *miR-34a* alone might be more apparent in a sensitized genetic background where this p53 redundancy is compromised.

Using this rationale, we disrupted the integrity of the p53 pathway in the *Kras*<sup>LSL-G12D</sup> model by introducing a deletion of one p53 allele. Although p53 acts as a haploinsufficient tumor suppressor in many cell types, p53 hemizygosity in *Kras*<sup>LSL-G12D</sup> mice did not significantly promote lung adenocarcinoma development (Supplemental Fig. S1E). The resulting *Kras*<sup>LSL-G12D/+</sup>; p53<sup>+/-</sup> mice phenocopied the *Kras*<sup>LSL-G12D/+</sup> mice in tumor latency, tumor size, and tumor grade, indicating that p53 hemizygosity did not preclude the p53 tumor suppressor effects in response to *Kras*-induced tumorigenesis. Con-

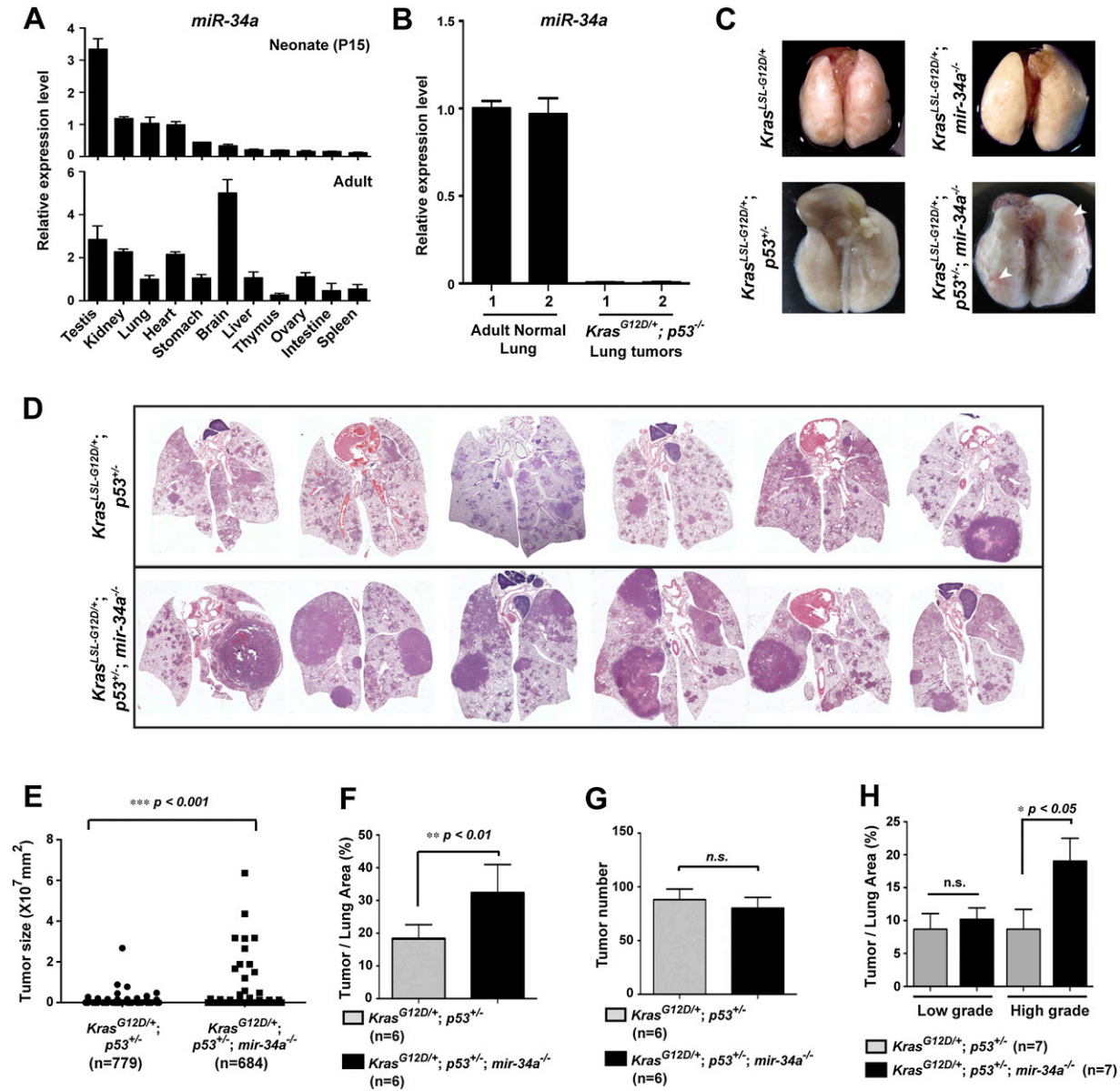


**Figure 1.** *miR-34a* deficiency and *p53* haploinsufficiency significantly promote *Kras*<sup>G12D</sup>-induced oncogenesis in lung adenocarcinomas. (A) *miR-34a* expression levels were measured by real-time PCR analyses in various organs of neonatal (postnatal day 15 [P15]; top) and adult (5 wk; bottom) mice. (B) *miR-34a* expression was readily detected in normal adult lungs but significantly reduced in *Kras*<sup>G12D/+</sup>; *p53*<sup>-/-</sup> lung adenocarcinomas. (C) The representative lung images are shown from *Kras*<sup>LSL-G12D/+</sup> and *Kras*<sup>LSL-G12D/+</sup>; *mir-34a*<sup>-/-</sup> mice 22 wk after AdCre infection (top) and *Kras*<sup>LSL-G12D/+</sup>; *p53*<sup>+/-</sup> and *Kras*<sup>LSL-G12D/+</sup>; *p53*<sup>+/-</sup>; *mir-34a*<sup>-/-</sup> mice 19 wk after AdCre infection (bottom). White arrowheads indicate the lung adenomas or adenocarcinomas on the lung surface. (D) Hematoxylin and eosin (H&E) staining of lung sections indicated a significant increase in tumor burden of *Kras*<sup>LSL-G12D/+</sup>; *p53*<sup>+/-</sup>; *mir-34a*<sup>-/-</sup> mice when compared with *Kras*<sup>LSL-G12D/+</sup>; *p53*<sup>+/-</sup> control mice. (E) Quantification of 779 *Kras*<sup>G12D/+</sup>; *p53*<sup>+/-</sup> and 684 *Kras*<sup>G12D/+</sup>; *p53*<sup>+/-</sup>; *mir-34a*<sup>-/-</sup> lung tumors demonstrated that a significant increase in tumor size was caused by *miR-34a* deficiency. (F) A significant increase in tumor burden was observed in *Kras*<sup>LSL-G12D/+</sup>; *p53*<sup>+/-</sup>; *mir-34a*<sup>-/-</sup> mice when compared with *Kras*<sup>LSL-G12D/+</sup>; *p53*<sup>+/-</sup> mice. The tumor burden was measured as the percentage of the tumor area versus the total lung area in six pairs of animals. (G) The tumor numbers in *Kras*<sup>LSL-G12D/+</sup>; *p53*<sup>+/-</sup> and *Kras*<sup>LSL-G12D/+</sup>; *p53*<sup>+/-</sup>; *mir-34a*<sup>-/-</sup> mice were similar ( $n = 6$ ). (H) The percentage of tumor area versus the total lung area was measured for low-grade (grades 1 and 2) and high-grade (grades 3–5) tumors in *Kras*<sup>LSL-G12D/+</sup>; *p53*<sup>+/-</sup> and *Kras*<sup>LSL-G12D/+</sup>; *p53*<sup>+/-</sup>; *mir-34a*<sup>-/-</sup> mice ( $n = 7$ ). While the tumor burden for low-grade tumors was similar for both genotypes, the tumor burden for high-grade tumors was significantly increased as a result of *miR-34a* deficiency. All analyses described in D–H were performed using mice at 19 wk after AdCre infection. All error bars represent SEM; (n.s.) not significant; (\*)  $P < 0.05$ ; (\*\*)  $P < 0.01$ ; (\*\*\*)  $P < 0.001$ .

sistently, we did not observe any *p53* loss of heterozygosity (LOH) in high-grade lung tumors derived from the *Kras*<sup>LSL-G12D</sup>; *p53*<sup>+/-</sup> mice (Supplemental Fig. S1F). These

findings suggest that in the *Kras*<sup>G12D</sup>-driven lung adenocarcinoma model, one allele of wild-type *p53* is sufficient to sustain *p53*-dependent tumor suppressor response.

Despite the similarities between *Kras*<sup>LSL-G12D/+</sup> and *Kras*<sup>LSL-G12D/+</sup>; *p53*<sup>+/-</sup> mice and MEFs (Supplemental Fig. S1E,G), complete *p53* deficiency significantly promotes *Kras*<sup>G12D</sup>-driven lung tumors (Jackson et al. 2005), suggesting that a strong oncogenic effect could occur in this model when the *p53* activity is below a critical threshold. Thus, compared with *Kras*<sup>G12D/+</sup> mice that have intact *p53* activity, *Kras*<sup>LSL-G12D/+</sup>; *p53*<sup>+/-</sup> animals are likely more susceptible to malignant transformation upon further disruption of the *p53* pathway, such as deficiency of *miR-34* miRNAs.

Interestingly, *miR-34a* deficiency strongly promoted the development of *Kras*<sup>G12D</sup>-induced lung adenocarcinoma in combination with *p53* hemizyosity, giving rise to mice with considerable respiratory difficulty or respiratory failure at 19 wk after AdCre exposure (Fig. 1C,D). At 19 wk, the lungs of *Kras*<sup>LSL-G12D/+</sup>; *p53*<sup>+/-</sup> control mice had a cobblestone appearance, with multiple small lesions on the lung surface; the lungs of *Kras*<sup>LSL-G12D/+</sup>; *p53*<sup>+/-</sup>; *mir-34a*<sup>-/-</sup> mice displayed multiple large tumors on the lung surface (Fig. 1C). Further histological analyses comparing *Kras*<sup>LSL-G12D/+</sup>; *p53*<sup>+/-</sup>; *mir-34a*<sup>-/-</sup> and control *Kras*<sup>LSL-G12D/+</sup>; *p53*<sup>+/-</sup> mice revealed increased tumor area and tumor size (Fig. 1D-F), yet the overall tumor numbers remained the same (Fig. 1G). Interestingly, *Kras*<sup>LSL-G12D/+</sup>; *p53*<sup>+/-</sup>; *mir-34a*<sup>-/-</sup> mice exhibited enhanced tumor area and increased tumor number of high-grade tumors but had little effect on the tumor area or number of low-grade tumors in the lung (Fig. 1H; Supplemental Fig. S1H). The high-grade tumors identified in *Kras*<sup>LSL-G12D/+</sup>; *p53*<sup>+/-</sup>; *mir-34a*<sup>-/-</sup> mice were often characterized by their large tumor size, large and pleomorphic nuclei, and high degree of stromal desmoplasia (Supplemental Fig. S1I). These findings suggest that when the robustness of the *p53* response is compromised, *miR-34a* deficiency leads to a significant acceleration in tumor progression of *Kras*<sup>G12D</sup>-driven lung adenocarcinomas.

We carried out a detailed histological analysis to determine the cell type of transformed cells in *Kras*<sup>LSL-G12D/+</sup>; *p53*<sup>+/-</sup>; *mir-34a*<sup>-/-</sup> mice. The adenomas and adenocarcinomas developed in *Kras*<sup>LSL-G12D/+</sup>; *p53*<sup>+/-</sup> and *Kras*<sup>LSL-G12D/+</sup>; *p53*<sup>+/-</sup>; *mir-34a*<sup>-/-</sup> mice were largely positive for surfactant apoprotein-C (SP-C), a marker for alveolar type II pneumocytes, and negative for CC10, a marker for Clara cells (Fig. 2A). Thus, these tumors arose from alveolar type II pneumocytes or their precursors. Since acute *miR-34a* overexpression reduced cell proliferation in the *Kras*<sup>G12D/+</sup>; *p53*<sup>R172H</sup> lung tumors (Kasinski and Slack 2012), we examined the effect of *miR-34a* deficiency on cell proliferation. Lung tumors in the *Kras*<sup>LSL-G12D/+</sup>; *p53*<sup>+/-</sup>; *mir-34a*<sup>-/-</sup> mice harbored increased numbers of Ki67-positive cells compared with those from the *Kras*<sup>LSL-G12D/+</sup>; *p53*<sup>+/-</sup> mice (Fig. 2B). This observation was consistent with a moderately increased cell proliferation seen in *miR-34a*-deficient MEFs after serial passages (Lal et al. 2011; Concepcion et al. 2012; data not shown). This enhanced cell proliferative phenotype associated with *miR-34a* deficiency likely contributed to the increased tumor progression for the high-grade tumors.

High-grade lung adenocarcinomas are often associated with enhanced MAPK signaling (Feldser et al. 2010). Compared with the control *Kras*<sup>LSL-G12D/+</sup>; *p53*<sup>+/-</sup> mice, the *Kras*<sup>LSL-G12D/+</sup>; *p53*<sup>+/-</sup>; *mir-34a*<sup>-/-</sup> mice developed more tumors that exhibited positive staining for phospho-Erk (p-Erk) (Fig. 2C). Previous studies suggested that the enhanced p-Erk signaling in high-grade *Kras*<sup>G12D</sup>-induced tumors invariably enhanced Arf expression, thus triggering potent *p53*-dependent tumor suppression to repress tumor progression (Feldser et al. 2010; Junttila et al. 2010). This enhanced *p53* signaling in high-grade *Kras*<sup>G12D</sup>-driven lung adenocarcinomas could, at least in part, counteract the enhanced MAPK signaling, thus delaying tumor progression (Feldser et al. 2010; Junttila et al. 2010). Since *miR-34a* is an integral component of the *p53* pathway, the specific increase of high-grade tumors in *Kras*<sup>LSL-G12D/+</sup>; *p53*<sup>+/-</sup>; *mir-34a*<sup>-/-</sup> mice may reflect a compromised *p53* activity in response to the aberrant MAPK signaling. Consistent with this hypothesis, *Kras*<sup>G12D/+</sup>; *p53*<sup>+/-</sup>; *mir-34a*<sup>-/-</sup> lung tumors, when compared with *Kras*<sup>G12D/+</sup>; *p53*<sup>+/-</sup> controls, exhibited a significant decrease in the induction of canonical *p53* targets, such as p21 (Fig. 2D,E). Not only was the percentage of tumors with high p21 expression significantly decreased, the average percentage of p21-positive cells within each tumor was also decreased (Fig. 2D,E). Similarly, we also observed a decrease in *p53* staining in *Kras*<sup>G12D/+</sup>; *p53*<sup>+/-</sup>; *mir-34a*<sup>-/-</sup> high-grade lung tumors, but not in low-grade ones, compared with *Kras*<sup>G12D/+</sup>; *p53*<sup>+/-</sup> controls (Supplemental Fig. S1J). Taken together, in the context of *p53* hemizyosity, the loss of *miR-34a* yielded a compromised *p53* response that failed to effectively antagonize the aberrant MAPK signaling in high-grade tumors, thus accelerating the tumor progression specifically in the high-grade lung tumors.

#### *p53* and *miR-34* miRNAs form a positive feedback loop

As bona fide *p53* targets, *miR-34* miRNAs also form a positive feedback loop with *p53*, which in turn regulates the degree of *p53* activation (Yamakuchi et al. 2008; Hermeking 2009). In both tumor cells and primary MEFs, the extent of cell cycle arrest induced by *miR-34* miRNAs was heavily dependent on the *p53* status. Enforced expression of *miR-34* miRNAs significantly induced the G1 arrest in HCT116 cells harboring wild-type *p53*; however, this anti-proliferative effect of *miR-34* was greatly dampened in *p53*<sup>-/-</sup> HCT116 cells (Fig. 3A). Similarly, overexpression of *pri-miR-34a* and *pri-miR-34b/34c* in wild-type MEFs induced a robust G1 arrest and a strong decrease in the S-phase population (Fig. 3B), yet only a small effect was observed when *p53*<sup>-/-</sup> MEFs were subjected to the same treatment (Fig. 3B). Notably, *miR-34* overexpression can still induce a mild G1 arrest in the *p53*-deficient cells (Fig. 3A,B), presumably due to the inhibition of cell cycle regulators such as CCND1, CDK4, and CDK6 (Supplemental Fig. S2C). Since *p53* is crucial for the cell cycle arrest effect induced by *miR-34*, we examined the effects of *miR-34* on *p53* activity. Forced expression of *miR-34* miRNAs increased the accumula-

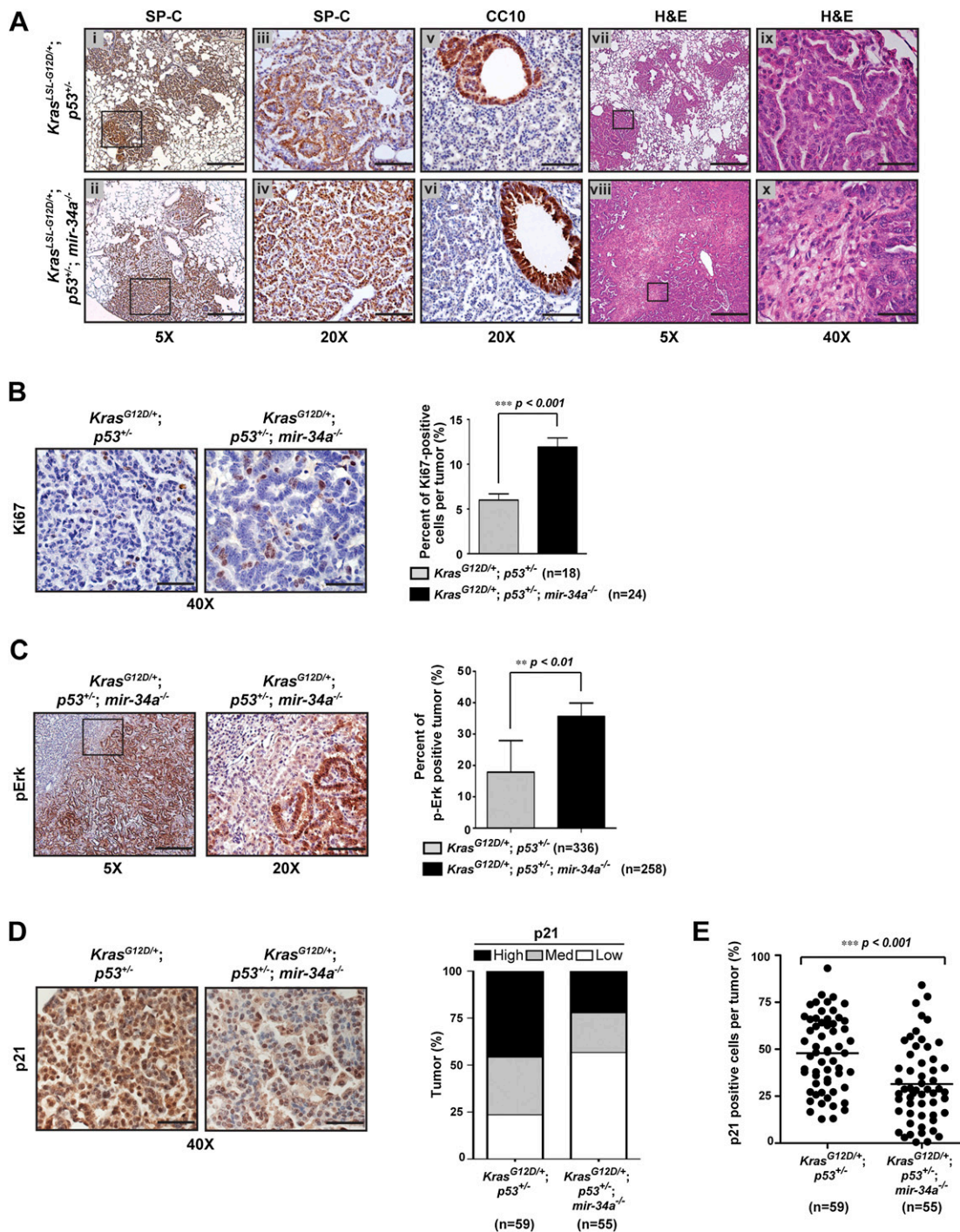


**Figure 2.** Histopathological analysis of lung tumors of *Kras<sup>LSL-G12D/+</sup>; p53<sup>+/-</sup>; mir-34a<sup>-/-</sup>* mice. (A) The lung adenomas and adenocarcinomas from the *Kras<sup>LSL-G12D/+</sup>; p53<sup>+/-</sup>* and *Kras<sup>LSL-G12D/+</sup>; p53<sup>+/-</sup>; mir-34a<sup>-/-</sup>* mice were derived from the alveolar type II pneumocytes. Lung sections from both genotypes were stained with SP-C (a marker for alveolar type II cells; panels *i-iv*), CC10 (a marker for Clara cells; panels *v* and *vi*), and H&E (panels *vii-x*). Bars: 5× images, panels *i,ii,vii,viii*, 400 μm; 20× images, panels *iii,iv,v,vi*, 100 μm; 40× images, panels *ix,x*, 50 μm. (B) *Kras<sup>G12D/+</sup>; p53<sup>+/-</sup>; mir-34a<sup>-/-</sup>* lung tumors contained a greater percentage of proliferating cells compared with *Kras<sup>G12D/+</sup>; p53<sup>+/-</sup>* tumors. Representative images (left) and quantitation (right) of Ki67 staining are shown for *Kras<sup>G12D/+</sup>; p53<sup>+/-</sup>* (n = 18) and *Kras<sup>G12D/+</sup>; p53<sup>+/-</sup>; mir-34a<sup>-/-</sup>* (n = 24) tumors stained with Ki67, a cell proliferation marker. Bars, 50 μm. (C) *Kras<sup>LSL-G12D/+</sup>; p53<sup>+/-</sup>; mir-34a<sup>-/-</sup>* mice carried a greater percentage of p-Erk-positive lung tumors compared with *Kras<sup>LSL-G12D/+</sup>; p53<sup>+/-</sup>* mice. Representative images (left) and quantitation (right) of p-Erk staining are shown. Bars: 5× images, 400 μm; 20× images, 100 μm. (D) *Kras<sup>G12D/+</sup>; p53<sup>+/-</sup>; mir-34a<sup>-/-</sup>* lung tumors exhibited a decreased p21 staining compared with *Kras<sup>G12D/+</sup>; p53<sup>+/-</sup>* tumors. Representative images of p21 staining are shown for both genotypes (left), and the classification of lung tumors was performed for both genotypes by the degree of p21 expression (right). Bars, 50 μm. (E) The percentage of p21-positive cells per tumor was calculated for 59 *Kras<sup>G12D/+</sup>; p53<sup>+/-</sup>* and 55 *Kras<sup>G12D/+</sup>; p53<sup>+/-</sup>; mir-34a<sup>-/-</sup>* lung tumors. All analyses were performed using mice 19 wk after AdCre infection. Error bars represent SEM; (\*\*)  $P < 0.01$ ; (\*\*\*)  $P < 0.001$ .

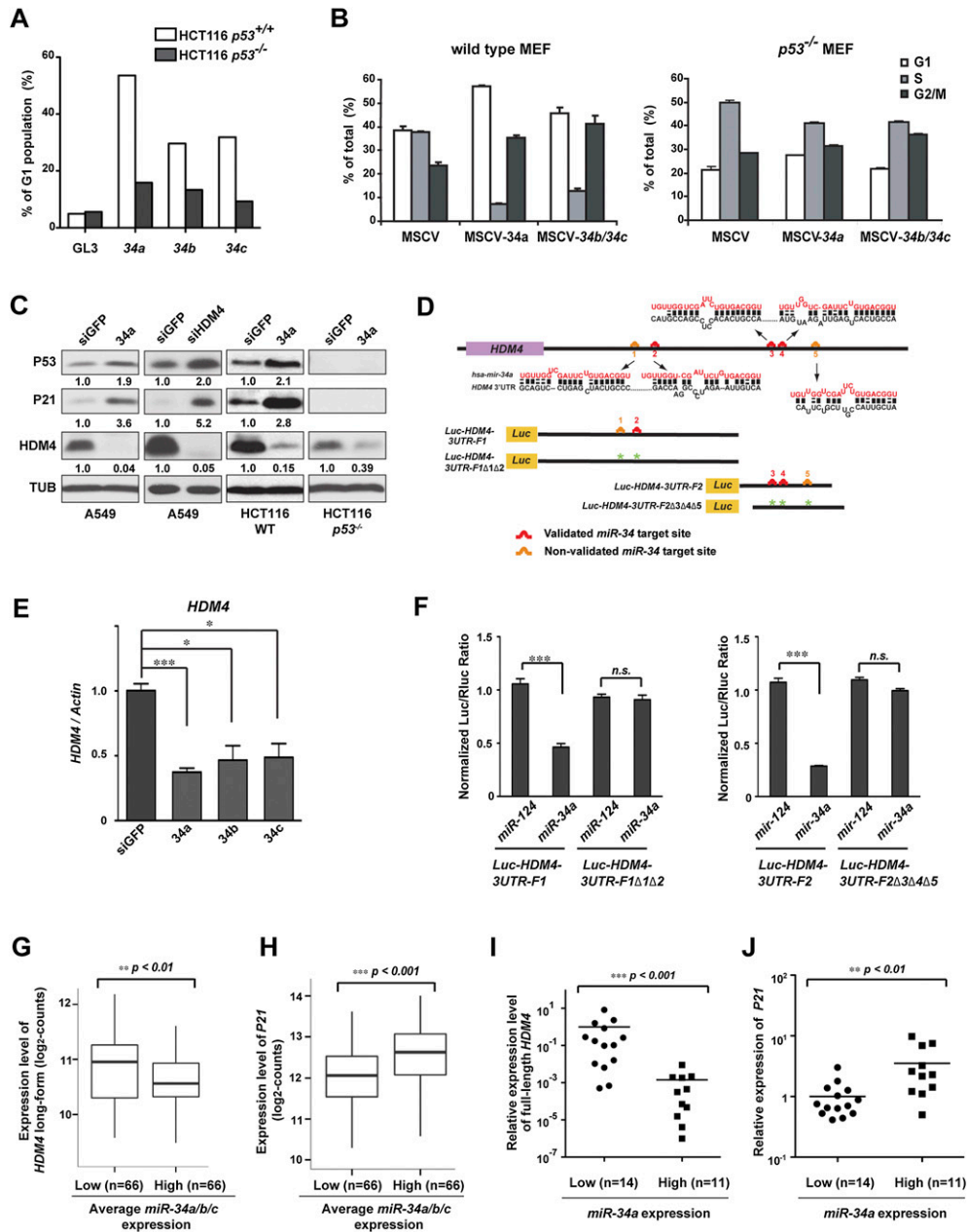


**Figure 3.** *miR-34* enhances p53 activity by post-transcriptional repression of HDM4. (A) The ability of *miR-34* to induce G1 cell cycle arrest greatly depends on an intact p53.  $p53^{+/+}$  or  $p53^{-/-}$  HCT116 cells were transfected with control siRNA (siGL3), *miR-34a*, *miR-34b*, or *miR-34c* and then treated with 100 ng/mL nocodazole to arrest cells in M phase. The percentage of G1 population in each transfection experiment was determined by flow cytometry. *miR-34* enhanced G1 cell cycle arrest in  $p53^{+/+}$  HCT116 cells, but this effect was significantly reduced in  $p53^{-/-}$  HCT116 cells. (B) *miR-34* overexpression reduced the S-phase population in wild-type MEFs (left panel), but this effect was significantly reduced in  $p53^{-/-}$  MEFs (right panel). Error bars are SD. (C) *miR-34a* and siHDM4 overexpression in A549,  $p53^{+/+}$ , and  $p53^{-/-}$  HCT116 cells significantly repressed the protein level of HDM4. *miR-34a* and siHDM4 overexpression in tumor cells with wild-type p53 caused a strong increase in p21 and a moderate increase in p53 protein level. (D, top) A schematic illustration of the full-length *HDM4* 3' UTR and the predicted *miR-34a*-binding sites. (Bottom) Luciferase reporters were constructed to test the predicted *miR-34a*-binding sites. Two fragments of *HDM4* 3' UTR (*HDM4*-3UTR-F1 and *HDM4*-3UTR-F2) were each cloned downstream from a luciferase reporter (Luc). All predicted *miR-34a*-binding sites in *HDM4*-3UTR-F1 or *HDM4*-3UTR-F2 (shown in red) were mutated in the luciferase reporter constructs (designated with asterisks). The *miR-34a*-binding sites validated in luciferase assays are labeled in red, while those that failed to have an effect are labeled in orange. (E) *miR-34* overexpression in A549 cells significantly reduced the mRNA level for *HDM4*. (F) In HCT116 *dicer*<sup>-/-</sup> cells, *miR-34a* specifically repressed luciferase reporters that carried *HDM4* *HDM4* 3' UTR fragments with intact *miR-34a*-binding sites. This *miR-34a*-dependent repression was abolished when the predicted *miR-34a*-binding sites in the *HDM4* 3' UTR fragments were mutated. (G,H) In human lung adenocarcinomas from the TCGA collection, expression of *HDM4* (G) and *P21* (H) exhibited inverse and positive correlation with the level of *miR-34* miRNAs, respectively. The expression level for *miR-34* for each sample was calculated as the average expression (log<sub>2</sub> counts) of *miR-34a*, *miR-34b*, and *miR-34c*. The tumor samples were categorized into "*miR-34* low" and "*miR-34* high" groups by using the 20% of the samples that had the lowest and highest expression value, respectively. Expression of *HDM4* (G) and *P21* (H) were compared among the "*miR-34* low" and "*miR-34* high" groups. The average expression of *miR-34* in the "*miR-34* high" group was >16-fold greater than that in the "*miR-34* low" group. (I,J) In a separate cohort of 25 lung adenocarcinoma samples, real-time PCR analyses confirmed the inverse correlation between *HDM4* and *miR-34a* (I) and the positive correlation between *P21* and *miR-34a* (J). Error bars represent SEM unless indicated otherwise. (\*)  $P < 0.05$ ; (\*\*)  $P < 0.01$ ; (\*\*\*)  $P < 0.001$ .

tion of p53 protein in several tumor cell lines and in primary MEFs carrying the wild-type *p53* (Fig. 3C; Supplemental Figs. S1G, S2A); increased p53-mediated transcription was confirmed by the induction of several canonical p53 targets, such as p21 (Fig. 3C; Supplemental Fig. S2A,B; data not shown). The induction of p21 by *miR-34a* depended on an intact p53, as no p21 induction was observed in *p53*<sup>-/-</sup> cells overexpressing *miR-34a* (Fig. 3C). Our results were consistent with a previous report indicating that the ability of *miR-34* miRNAs to induce apoptosis in HCT116 cells depended on the presence of an intact p53 (Raver-Shapira et al. 2007; Yamakuchi et al. 2008). These findings suggest that p53 and *miR-34* form a positive feedback loop to strengthen the downstream effects of p53. Thus, disruption of this positive feedback loop could significantly compromise the p53 tumor suppressor response.

This *p53-miR-34* positive feedback could at least in part explain why the oncogenic effect of *miR-34a* deficiency in vivo was dependent on the p53 status. Deficiency of *miR-34a* disrupts the *p53-miR-34* positive feedback, which could be compensated for by the redundancy of an intact p53 pathway in vivo. However, when p53 was haploinsufficient, *miR-34a* deficiency in *Kras*<sup>LSL-G12D/+</sup>; *p53*<sup>+/-</sup>; *mir-34a*<sup>-/-</sup> mice further disrupted the robustness of the p53 response, possibly creating a p53 activity that was below a critical threshold for maintaining adequate tumor suppression in vivo. Similarly, *miR-34a* deficiency in *Kras*<sup>G12D/+</sup>; *p53*<sup>+/-</sup> MEFs compromised the extent of p53 activation in response to the activating *Kras* mutation (Supplemental Fig. S2D). Thus, the oncogenic effect conferred by *miR-34a* deficiency is dependent on the *p53* status.

#### *miR-34* represses *Mdm4* to activate p53 and establish a positive feedback loop

A previous report indicated that *miR-34* miRNAs promoted p53-mediated apoptosis in vitro by positively regulating p53 acetylation (Yamakuchi et al. 2008). This is at least in part attributed to the ability of *miR-34* miRNAs to directly repress SIRT1, which deacetylates p53 to impede p53-mediated transactivation (Yamakuchi et al. 2008). Although we confirmed the direct inhibition of *SIRT1* by *miR-34* overexpression in multiple tumor cell lines (Supplemental Fig. S2E,F), we did not observe any inverse correlation between *miR-34* and *SIRT1* in human lung adenocarcinomas using RNA sequencing (RNA-seq) data from The Cancer Genome Atlas project (TCGA) (data not shown). Thus, at least in the context of lung tumor development, additional mechanisms could mediate the positive feedback between p53 and *miR-34*.

To identify additional *miR-34* targets that mediate its positive regulation of p53 activity, we focused on negative regulators of p53 that contain predicted *miR-34* target sites in their 3' untranslated regions (UTRs). Our analysis employed both computational predictions (TargetsScan and RNA22) (Lewis et al. 2003; 2005; Miranda et al. 2006; Grimson et al. 2007) and data mining in published *miR-34* pull-down data (Lal et al. 2011) and microarray

data (Chang et al. 2007). Among many reported putative *miR-34* targets, the *Mdm4* gene (also referred to as *HDM4* in humans) emerged as a prominent candidate due to the presence of multiple predicted *miR-34* target sites in the 3' UTR (Fig. 3D; Supplemental Fig. S2H) and its important functions as one major negative regulator of p53 (Marine et al. 2006; Markey and Berberich 2008; Mandke et al. 2012; Wade et al. 2013). *mdm4/HDM4* and its closely related homolog, *mdm2/HDM2*, both encode RING domain proteins that promote oncogenesis by inhibiting p53 (Marine et al. 2006; Wade et al. 2013). The negative regulation of p53 by Mdm4 is best demonstrated by the aberrant p53 activation in Mdm4-deficient mice, which causes embryonic lethality at embryonic day 10.5 (E10.5) (Parant et al. 2001; Migliorini et al. 2002). While Mdm2 acts as an ubiquitin E3 ligase that promotes p53 protein degradation via polyubiquitination (Eischen and Lozano 2009; Kruse and Gu 2009), Mdm4 does not possess E3 ubiquitin ligase activity by itself. In addition to repressing p53-dependent transactivation (Wade et al. 2013), Mdm4 positively regulates Mdm2 to promote p53 polyubiquitination, which leads to proteasomal degradation of p53 (Wang et al. 2011a).

Real-time PCR and Western analyses in a variety of mouse and human cell lines both indicated that endogenous Mdm4/HDM4 expression was subjected to the *miR-34*-dependent repression, with effects seen on both the transcript and protein levels (Fig. 3C,E; Supplemental Fig. S2I,J). The repression of HDM4 by *miR-34a* in p53 wild-type tumor cells was correlated with a moderate increase in p53 protein level and a strong induction of canonical p53 targets, such as p21 (Fig. 3C; Supplemental Fig. S2A). The moderate increase in p53 protein level was at least in part due to reduced ubiquitin-mediated proteasomal degradation (Supplemental Fig. S2G). Interestingly, the extent of p21 induction by *miR-34* was stronger than that of p53 protein increase (Fig. 3C; Supplemental Fig. S2A,E), suggesting that HDM4 modulates p53 activity in both a proteasome-dependent and proteasome-independent manner.

Using TargetsScan and RNA22, we predicted five *miR-34*-binding sites in the 3' UTR of the full-length *HDM4* transcript (Fig. 3D). Our luciferase reporter assays validated the functional importance of three of these predicted sites (Fig. 3F; Supplemental Fig. S2K). Luciferase reporters carrying the wild-type 3' UTR exhibited significant repression upon *miR-34* overexpression; mutation of selected *miR-34*-binding sites abolished this *miR-34*-dependent regulation (Fig. 3F; Supplemental Fig. S2K). In *miR-34* overexpression studies, the extent of HDM4 repression was comparable with or stronger than that seen for other well-characterized *miR-34* targets, including CCND1, CDK6, and SIRT1 (Fig. 3C; Supplemental Fig. S2C; Sun et al. 2008; Yamakuchi et al. 2008). In mice, *mdm4* could be transcribed into multiple isoforms in vivo, each of which was validated by 3'-RACE (data not shown). *miR-34* represses a long isoform of *mdm4* in mice, which contains four predicted *miR-34* target sites in its 3' UTR (Supplemental Fig. S2H,I; data not shown).

### Human lung adenocarcinomas express a short *HDM4* isoform that evades miR-34-mediated repression

Given the direct repression of *HDM4* by *miR-34* in vitro, we examined the correlation between *miR-34* miRNAs and *HDM4* in human lung adenocarcinomas. Using the RNA-seq data from TCGA, we observed an inverse correlation between the levels of full-length *HDM4* mRNAs and those of *miR-34* miRNAs in 327 lung adenocarcinomas (Fig. 3G). Not surprisingly, the *HDM4* level inversely correlated with the levels of canonical p53 targets, such as *P21* (Supplemental Fig. S3A). These findings were consistent with a positive correlation between the expression of *miR-34* miRNAs and that of the canonical p53 target, such as *P21*, in these samples (Fig. 3H). We observed a similarly strong correlation when we examined the expression of *miR-34* miRNAs and the expression of a cohort of validated p53 targets (Supplemental Fig. S3B). To validate our findings from TCGA data sets, we also collected 26 paired human lung adenocarcinomas and their normal adjacent controls and performed real-time PCR analyses to measure the expression levels of *HDM4*, *miR-34* miRNAs, and *P21*. Using this cohort of lung adenocarcinoma samples, we confirmed the existence of an inverse correlation between full-length *HDM4* and *miR-34* miRNAs (Fig. 3I; Supplemental Fig. S3C) as well as a positive correlation between *miR-34* miRNAs and *P21* (Fig. 3J; Supplemental Fig. S3D). Since *miR-34* miRNAs are p53 targets, the correlation between *miR-34* miRNAs and other p53 targets in human lung adenocarcinomas could also reflect the transcriptional activity of p53. Nevertheless, the inverse correlation between *miR-34* and *HDM4* and the ability of *miR-34* to directly repress *HDM4* and activate p53 strongly argue that the p53/*miR-34*/*HDM4* positive feedback could, at least in part, contribute to this correlation. Collectively, our findings support the importance of the p53–*miR-34* positive feedback during the development of lung adenocarcinomas.

Interestingly, *HDM4* encodes several isoforms in lung adenocarcinomas due to alternative polyadenylation. The full-length *HDM4* isoform is produced with an intact 3' UTR, while several *HDM4* isoforms are generated with a shorter 3' UTR that is devoid of all *miR-34*-binding sites (Fig. 4A). Although expression from the full-length *HDM4* mRNA is inhibited by *miR-34*, expression from the short *HDM4* isoforms largely evades *miR-34*-dependent regulation, as confirmed using luciferase reporter assays (Fig. 4B). In both TCGA data sets and our own cohort of lung adenocarcinoma samples, the shorter *HDM4* RNA isoforms accumulated to higher levels in lung adenocarcinomas compared with their adjacent normal tissues. Hence, increased ratios of short versus full-length *HDM4* RNA isoforms were seen in lung adenocarcinoma tissues (Fig. 4C, 4D). It is unclear how lung adenocarcinomas promote the alternative polyadenylation of the *HDM4* transcript. It is also unclear how the expression levels of the short *HDM4* isoforms compare with that of the full-length *HDM4*, yet the tumor-specific increase in the short *HDM4* RNA isoforms is

expected to permit bypassing of *miR-34*-dependent regulation of a subset of total *HDM4* transcripts. Thus, deregulation of *miR-34* or alternative *HDM4* polyadenylation can evade *miR-34*-mediated *HDM4* repression, thus dampening p53 response by disrupting the p53/*miR-34*/*HDM4* feedback (Fig. 4E). Taken together, our results elucidated the intricate cross-talk between p53 and *miR-34* miRNAs and revealed an important tumor suppressor effect generated by this positive feedback loop.

### Discussion

The pathways downstream from p53 exhibit extensive redundancy. The deficiency of canonical p53 targets rarely recapitulated the spectrum and the extent of the oncogenic defects caused by the deficiency of p53 itself. Although the p53-regulated *miR-34* miRNAs have been implicated as potent tumor suppressors, subsequent loss-of-function studies yielded a more complicated picture due to this p53 redundancy (Concepcion et al. 2012). Specifically, deletion of *mir-34a* and *mir-34b/34c* in MEFs caused little or no change in p53-mediated cell cycle arrest or apoptosis in vitro and caused no increase in tumorigenesis in vivo (Concepcion et al. 2012). The seemingly intact p53 response in *miR-34*-deficient cells and animals is not entirely surprising. It is conceivable that *miR-34* miRNAs are integral components of a robust yet highly redundant p53 tumor suppressor pathway. The loss of *mir-34a* and *mir-34b/34c* could initiate a compensatory pathway mediated by either redundant effectors downstream from p53 or homologous miRNAs that share the same/similar target specificity. It is also possible that the functional importance of the p53–*miR-34* axis is cell type-dependent and context-dependent, and the tumor suppressor effects of *miR-34* miRNAs might be more apparent in a specific biological context.

While p53 induces the transcription of *miR-34* miRNAs, these miRNAs in turn repress Mdm4 and/or Sirt1 post-transcriptionally to enhance p53 transcription activity and decrease p53 protein turnover. This positive feedback loop between p53 and *miR-34* further strengthens the p53 activity upon p53 activation, conferring a robust tumor suppression response. In the *Kras*-induced lung adenocarcinoma model, the highly redundant and robust p53 pathway could tolerate a moderate disruption, such as that caused by *miR-34a* deficiency alone or by p53 hemizyosity. However, *miR-34a* deficiency combined with p53 hemizyosity further disrupts the p53 pathway, causing the strength of the p53 activity to be below a critical threshold required for sufficient tumor suppression in vivo. Our results may seem paradoxical to a previous study, where *miR-34* deficiency in MEFs does not impact the p53-mediated cell cycle arrest and apoptosis in response to genotoxic stress (Concepcion et al. 2012). However, it is possible that the p53–*miR-34* positive feedback loop has little impact on the acute p53 response but does affect the p53 activation that is required for tumor suppression under sustained oncogenic stresses.

The tumor suppressor effects of *miR-34* in vivo could also be mediated through both p53-dependent and p53-

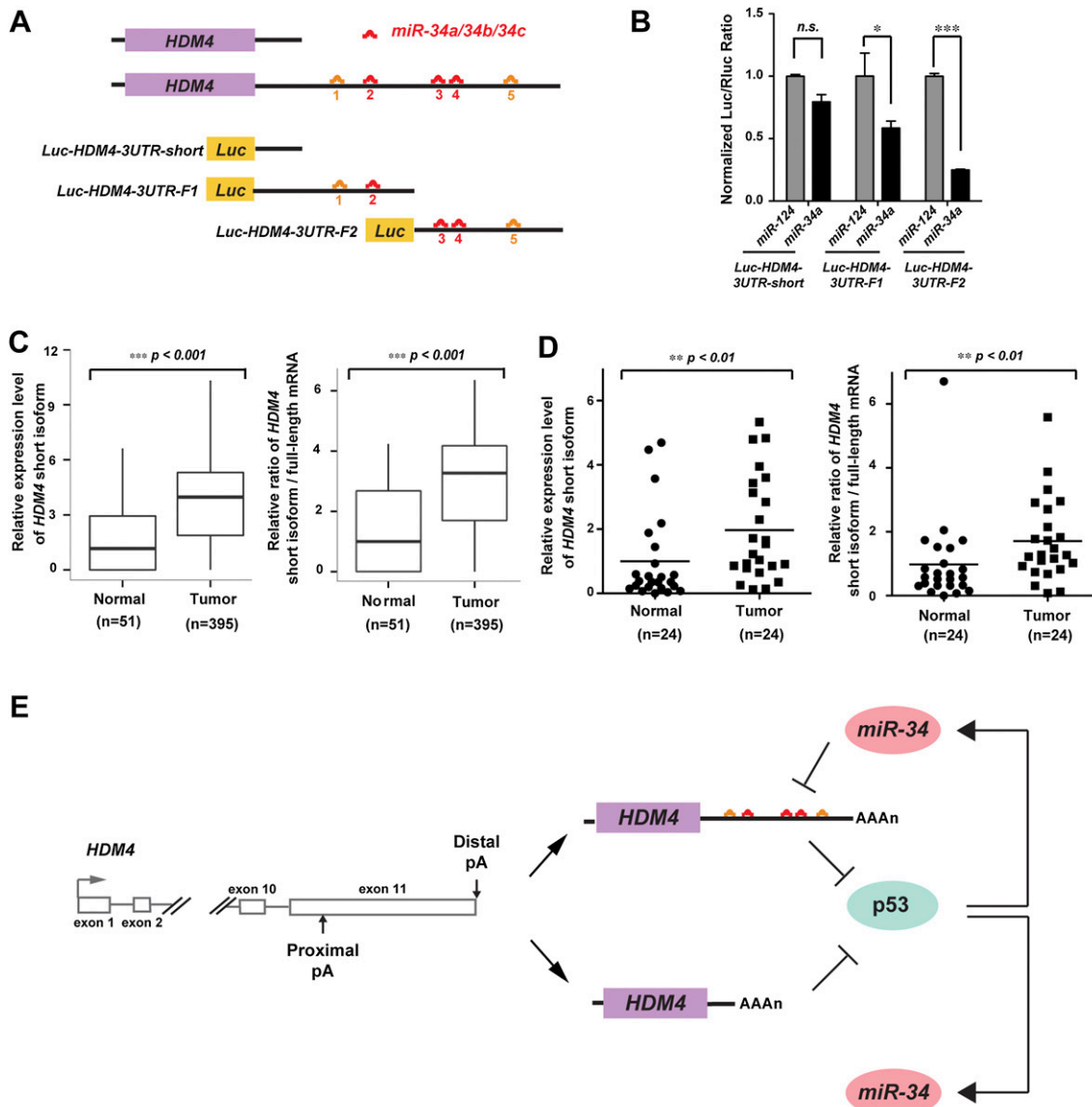


**Figure 4.** Human lung adenocarcinomas express a short *HDM4* isoform that evades *miR-34*-mediated repression. (A) A schematic illustration of the 3' UTRs of a short *HDM4* isoform and a full-length *HDM4*. The short *HDM4* isoform does not contain any predicted *miR-34*-binding sites in the 3' UTR. (B) The short *HDM4* isoform carries a 3' UTR that escapes *miR-34* regulation. In HCT116 *dicer*<sup>-/-</sup> cells, *miR-34a* overexpression mediated a strong repression of the luciferase reporters that carried the 3' UTR fragments from the full-length *HDM4*. However, *miR-34a* failed to alter the expression of the luciferase reporter that carried the 3' UTR from the short *HDM4* isoform. (C,D) Human lung adenocarcinomas exhibit a greater level of *HDM4* short isoforms (shown at left) and a greater ratio between short and full-length *HDM4* mRNAs. (C) The expression of *HDM4* short isoforms and full-length *HDM4* isoforms was calculated as log<sub>2</sub> counts in normal and tumor samples using the level III RNA-seq data from TCGA. (D) A similar comparison was performed using real-time PCR quantitation from a cohort of 24 paired lung adenocarcinoma and normal control samples. The average expression of the *HDM4* short isoform in normal samples was normalized to 1, and the average ratio between short and full-length *HDM4* mRNAs in normal samples was also normalized to 1. (E) A diagram describes our proposed model to explain the positive feedback between p53 and *miR-34* miRNAs and how alternative polyadenylation of *HDM4* could escape this feedback regulation. Error bars represent SEM. (\*\*)*P* < 0.01; (\*\*\*)*P* < 0.001.

independent mechanisms. Several studies have demonstrated that the *miR-34a* targets are enriched for components in the growth factor signaling and cell cycle progression (Lal et al. 2011). In particular, multiple candidate *miR-34a*-regulated genes, including c-Met and Axl, participate in the RAS-RAF-MAPK signaling (Lal et al. 2011). This is

consistent with the decreased Erk phosphorylation in *Kras*<sup>G12D/+</sup>; *p53*<sup>-/-</sup> tumor cell lines in response to *miR-34a* overexpression (data not shown). This is also consistent with the enhanced Erk phosphorylation in *Kras*<sup>G12D/+</sup>; *p53*<sup>+/-</sup>; *mir-34a*<sup>-/-</sup> tumors when compared with the *Kras*<sup>LSL-G12D/+</sup>; *p53*<sup>+/-</sup> controls. Increased MAPK signal-

ing in high-grade *Kras*<sup>G12D</sup>-driven lung tumors often triggers p53 activation to repress tumor progression. Thus, in the *Kras*<sup>LSL-G12D/+</sup>; *p53*<sup>+/-</sup>; *mir-34a*<sup>-/-</sup> mice, an increased MAPK signaling resulting from the activated *Kras*<sup>G12D</sup> and *miR-34a* deficiency combined with a dampened p53 response due to p53 hemizyosity and *miR-34a* deficiency could generate a strong oncogenic effect that we observed in vivo. Consistently, when comparing *Kras*<sup>LSL-G12D/+</sup>; *p53*<sup>+/-</sup>; *mir-34a*<sup>-/-</sup> tumors with *Kras*<sup>LSL-G12D/+</sup>; *p53*<sup>+/-</sup> tumors, a reduced p53 staining is evident in the high-grade tumors but not the low-grade tumors.

Our analysis of clinical samples implicates the functional significance of *miR-34*-dependent *HDM4* repression. It is likely that disrupting the p53/*miR-34*/*HDM4* feedback by *miR-34* deficiency or by alternative polyadenylation of *HDM4* could contribute to an increased oncogenesis in human lung adenocarcinomas. In two separate cohorts of lung adenocarcinomas, a strong inverse correlation exists between *miR-34* miRNAs and full-length *HDM4*, and a considerable positive correlation occurs between *miR-34* and canonical p53 targets. These results suggest that the disruption of the p53/*miR-34*/*HDM4* feedback could represent an important mechanism to dampen the p53-mediated tumor suppression. In human lung adenocarcinomas, multiple mechanisms can act to disrupt this p53/*miR-34*/*HDM4* feedback regulation. In addition to p53 mutations, deregulation of *miR-34* miRNAs through either genomic deletion or promoter hypermethylation occurs frequently in lung cancers (Tanaka et al. 2012). Furthermore, tumors exhibit an increased level of short *HDM4* isoforms that are devoid of all *miR-34*-binding sites to bypass *miR-34*-mediated repression. The tumor-specific increase in the short *HDM4* transcripts in human lung adenocarcinomas could constitute yet another mechanism to disrupt the p53–*miR-34* feedback regulation and, ultimately, contribute to tumor development.

In the p53 pathway, there are many positive and negative feedback loops whose biological effects are cell type-dependent and context-dependent. Here, we demonstrated that the p53–*miR-34* positive feedback constitutes an important regulation of the extent of tumor suppression during lung cancer development. This p53–*miR-34* positive feedback regulation fine-tunes the degree of p53 activation and connects the p53 pathway with other signaling pathways, conferring both redundancy and robustness to the p53 tumor suppressor network.

## Materials and methods

### Animals

Mice of *Kras*<sup>LSL-G12D/+</sup> genotype were crossed with *p53*<sup>+/-</sup> or *p53*<sup>-/-</sup>; *mir-34a*<sup>-/-</sup> mice to generate *Kras*<sup>LSL-G12D/+</sup>; *p53*<sup>+/-</sup> and *Kras*<sup>LSL-G12D/+</sup>; *p53*<sup>+/-</sup>; *mir-34a*<sup>-/-</sup> mice. Lung tumorigenesis was induced by intranasal incubation of  $2.5 \times 10^7$  plaque-forming units of recombinant AdCre virus (University of Iowa Gene Transfer Vector Core) in 8-wk-old mice.

### Isolation of mouse tumor cells

Cell lines were isolated from individual lung tumors recovered at necropsy. Following harvest, tumors were cut into small pieces

and digested for 30 min at 37°C in 2 mL of Hanks' buffered salt solution (HBSS) containing dispase (Invitrogen, no. 17105-041) and collagenase type IV (Invitrogen, no. 17104-019). Following digestion, ice-cold DNase (Roche Applied Science, no. 10104159001) was added, and the mixture was incubated for 10 min on ice. Digested tumor samples then were pressed through 40- $\mu$ m cell strainers. Finally, samples were centrifuged at 1000 rpm for 5 min at room temperature, resuspended in culture medium (DMEM; Invitrogen, no. 11995-073) supplemented with 10% fetal bovine serum (FBS) and 1% penicillin and streptomycin (Invitrogen, no. 15140-163), and plated in 12-well plates.

### Cell culture and transfection

MEFs and Phoenix-E cells were maintained in DMEM supplemented with 10% FBS and 1% penicillin and streptomycin. Primary *Kras*<sup>LSL-G12D/+</sup> MEFs with various genotypes were infected with AdCre virus by incubation for 12 h in DMEM supplemented with 2% FBS and 1% penicillin and streptomycin. A549 cells and primary mouse lung tumor-derived cells were maintained in RPMI1640 medium (Invitrogen, no. 11875-119) supplemented with 10% FBS and 1% penicillin and streptomycin. HCT116 cells were maintained in McCoy's 5A medium (Invitrogen, no. 16600-082) supplemented with 10% FBS and 1% penicillin and streptomycin. Transient transfection of HCT116 and A549 cells was performed using either Oligofectamine (Invitrogen, no. 12252-011) or Lipofectamine 2000 (Invitrogen, no. 11668-019) according to the manufacturer's instruction.

### Histopathology and immunohistochemistry (IHC)

For determining tumor incidence, area, and grade, whole lungs were fixed overnight in 10% buffered formalin (Fisher Scientific, no. SF100-4), dehydrated in a graded series of ethanol solutions, embedded in Paraplast X-TRA paraffin (Fisher Scientific, no. 23-021-401), sectioned at 6- $\mu$ m thicknesses, mounted on glass slides, and stained with hematoxylin and eosin (H&E) using standard procedures. Lung and tumor areas were determined using Image Viewer (Ventana Medical Systems/Roche). Tumors were analyzed on H&E sections. Each tumor was given a score of grade 1–5 (Jackson et al. 2005). Grades 1 and 2 were classified as low-grade tumors, and grades 3–5 were classified as high-grade tumors.

For IHC, paraffin sections were deparaffinized, dehydrated, and subjected to heat-induced antigen retrieval in a pressure cooker using 10 mM sodium citrate buffer (pH 6.0). Slides were incubated for 10 min with 3% H<sub>2</sub>O<sub>2</sub>, blocked for 3 h with 5% bovine serum albumin (BSA) in phosphate-buffered saline (PBS) containing 0.3% Triton X-100, and incubated with primary antibody overnight in 1% BSA in PBS-0.3% Triton X-100. Horseradish peroxidase (HRP)-conjugated secondary antibodies (Invitrogen, no. G-21234; Santa Cruz Biotechnology, no. sc-2768) were incubated for 2 h at room temperature, with a 1:400 dilution in PBS containing 5% BSA and 0.3% Triton X-100. For p-Erk and p21 staining, a biotinylated horse anti-rabbit secondary antibody (Jackson ImmunoResearch, no. 711-065-152) was used at 1:400 as above, followed by incubation with Vectastain elite ABC reagent (Vector Laboratories, no. PK7100) for 30 min. Peroxidase was then visualized by DAB staining (Invitrogen, no. 00-2014) and counterstaining with Mayer's hematoxylin (Electron Microscopy Sciences, no. 26503-04).

### Real-time PCR analyses

Total RNA was extracted from cells or tissues using Trizol (Invitrogen, no. 15596) according to the manufacturer's instruc-

tion. For miRNA real-time PCR assays, cDNA was synthesized from total RNA using the high-capacity cDNA reverse transcription kit (Applied Biosystems, no. 4368814). Subsequently, quantitative PCR was carried out using TaqMan miRNA assays (Applied Biosystems) to detect mature *miR-34* miRNA levels. For mRNA real-time PCR, cDNA was synthesized from total RNA using the iScript advanced cDNA synthesis kit (Bio-Rad, no. 170-8843), and mRNA expression levels were determined by real-time PCR with SYBR (Kapa Biosystems, no. KK4604). The primers used here are shown in Supplemental Table S1.

### 3'-end real-time PCR

Total RNA was extracted from cells or tissues using Trizol according to the manufacturer's instruction. RNA was heat-fragmented for 5 min at 70°C with the RNA fragmentation reagent (Ambion, no. AM8740). The fragmented RNA was precipitated and then used to synthesize cDNA by RT-PCR with SuperScript III reverse transcriptase (Invitrogen, no. 18080044). mRNA expression levels were determined by real-time-PCR with SYBR. The primers used here are shown in Supplemental Table S1.

### 3'-RACE

The 3'-RACE was performed using mouse testis marathon-ready cDNA (Clontech, no. 639405) according to the manufacturer's protocol. We cloned multiple *mdm4* isoforms with different lengths of 3' UTRs. The longest *mdm4* isoform, validated by RT-PCR, contains a 3' UTR of 5435 nucleotides, which harbors four predicted *miR-34* target sites.

### Western blot analysis

Total cellular extracts resolved by SDS-PAGE were transferred to nitrocellulose filters. Western blotting was performed in TBST (100 mM Tris-HCl at pH 7.5, 150 mM NaCl, 0.05% Tween-20) containing 5% nonfat milk or 5% BSA. Immunoreactive protein bands were visualized by using Pierce ECL Western blotting substrate (Thermo Scientific, no. 32106).

### Antibodies

The following monoclonal (mAb) and polyclonal (pAb) primary antibodies were used for immunoblotting and IHC: SIRT1 pAb (1:1000; Abcam, no. ab13749), HDM4 pAb (1:1000; Bethyl Laboratories, no. A300-287A), p53 mAb (1:1000; Cell Signaling, no. 2524), pErk mAb (1:1000 [Cell Signaling, no. 4370] for immunoblotting; 1:75 [Cell Signaling no. 4376] for IHC); HDM4 mAb (1:1000; Millipore, no. 04-1555), p53 mAb (1:1000; Millipore, no. OP43), surfactant protein C pAb (1:200; Millipore, no. AB3786); CC10 pAb (1:400; Santa Cruz, no. sc-25555), p21 mAb or pAb (1:100 [Santa Cruz, no. sc-6246] for immunoblotting; 1:100 [Santa Cruz, sc-471] for IHC),  $\alpha$ -tubulin mAb (1:5000; Sigma, no. T5168), and Ki67 mAb (1:200; Thermo Scientific, no. RM-9106-S1).

### Ubiquitination assay

For the ubiquitination assay, HCT116 cells on one 10-cm plate were cotransfected with 25 nM RNA oligos (siGFP or *miR-34a* mimics), 4  $\mu$ g of HA-ubiquitin plasmid, and 1  $\mu$ g of pcDNA-p53 plasmid using Lipofectamine 2000 (Invitrogen) following the manufacturer's protocol. Cells were treated with 20  $\mu$ M MG132 (Sigma, no. C2211) 4 h before harvesting. Forty-eight hours after transfection, cells were lysed in standard RIPA buffer

(10 mM Tris at pH 8.0, 1% NP-40, 2 mM EDTA, 150 mM NaCl with the Roche protease inhibitor, no. 11697498001), and the whole-cell lysates were subjected to immunoprecipitation with 2  $\mu$ g of anti-p53 (FL-393-G, Santa Cruz Biotechnology) antibody and protein A/G agarose (Pierce). The immunoprecipitates were immunoblotted with anti-HA antibody (1:1000; Santa Cruz Biotechnology, no. 12CA5) to detect the ubiquitinated p53.

### Plasmid DNA constructs

Three fragments corresponding to the *HDM4* 3' UTR were amplified by PCR using human genomic DNA as a template with the primers shown in Supplemental Table S1. Fragments 1 and 2 (F1 and F2) were cloned downstream from a luciferase reporter in a pGL3 vector (Promega, no. E1751). Seed regions were mutated to remove all complementarity to *miR-34* miRNAs by QuickChange mutagenesis kit (Stratagene) with the primers shown in Supplemental Table S1. The short form of the *HDM4* 3' UTRs was similarly cloned into the same luciferase reporter vector.

### Luciferase assay

HCT116 *Dicer*<sup>-/-</sup> cells were cotransfected with 100 ng of reporter constructs and 50 nM miRNAs (*miR-34a* or *miR-124a*) in the form of siRNA using LT1 (Mirus, no. MIR2300) and TKO (Mirus, no. MIR2150). Ten nanograms of pRLTK (Promega, no. E2241) also was cotransfected as a normalization control. Cells were lysed 48 h after transfection, and ratios between firefly and *Renilla* luciferase activity were measured with the dual-luciferase reporter assay system (Promega, no. E1910).

### Gene expression analysis of the TCGA data set

For the TCGA data set, miRNA-seq and RNA-seq data were generated using an Illumina HiSeq 2000 sequencing platform from lung adenocarcinoma samples and normal adjacent controls. The read counts were already summarized for each miRNA or mRNA isoform, and the expression level of each gene can be retrieved from the TCGA level 3 data (archives bcgsc.ca\_LUAD. IlluminaHiSeq\_miRNASeq.Level\_3.1.4.0 and unc.edu\_LUAD. IlluminaHiSeq\_RNASeqV2.Level\_3.1.8.0).

For miRNA-seq data, we summarized the miRNA-seq data at the level of the MIMATs (miRNA IDs) and selected 631 miRNAs that have at least five read counts in at least 5% of the samples. The raw counts were normalized using upper-quantile. The plate 1757, which contained seven normal samples, constituted a batch different from the other normal samples and was not included in the analysis of the miRNA-seq data.

For RNA-seq data, the read counts already summarized at the gene and transcript levels were retrieved from the TCGA level 3 data (archive unc.edu\_LUAD.IlluminaHiSeq\_RNASeqV2.Level\_3.1.8.0). RSEM was used to estimate gene and transcript abundance. Eighteen-thousand-three-hundred-eighteen genes and 59,847 transcripts with at least five counts in at least 5% of the samples were selected. The raw counts were then normalized using upper-quantile. Three *HDM4* transcripts carried an intact 3' UTR (uc001hba.2, uc001hbb.2, and uc001hbc.2), and two short *HDM4* transcripts carried a short 3' UTR devoid of all *miR-34*-binding sites (uc010pqw.1 and uc010pqx.1). Their counts were summed up to get one expression value per sample for the *HDM4* long and short forms, respectively. The RNA-seq data included 395 tumor samples and 51 adjacent normal controls, of which 327 tumor and 12 adjacent normal samples were also available in the miRNA-seq data.

## Acknowledgments

We thank members of the He laboratory for their help and input. Particularly, we thank S. Nishimura, M.R. Junttila, M. McMahon, M. Winslow, M.J. Bennett, J. Shue, S.K. Greaney, K. Hou, D. Yang, and Y.J. Choi for technical assistance and stimulating discussions. We also thank P. Margolis helpful advice on manuscript preparation. We thank B. Zaghi and J. Ong for the technical assistance. L.H. is a Searle Scholar supported by the Kinship Foundation. L.H. also acknowledges the support of an R01 and an R21 grant from the National Cancer Institute (NCI; R01 CA139067 and 1R21CA175560-01), a research scholar award from American Cancer Society (ACS; 123339-RSG-12-265-01-RMC), and a research grant from The Tobacco-Related Disease Research Program (TRDRP; 21RT-0133). C.-P.L. is supported by a post-doctoral fellowship from the California Institute for Regenerative Medicine (CIRM) and a post-doctoral fellowship from the Siebel Foundation.

## References

- Ambros V. 2004. The functions of animal microRNAs. *Nature* **431**: 350–355.
- Bartel DP. 2009. MicroRNAs: Target recognition and regulatory functions. *Cell* **136**: 215–233.
- Chang T-C, Wentzel EA, Kent OA, Ramachandran K, Mullendore M, Lee KH, Feldmann G, Yamakuchi M, Ferlito M, Lowenstein CJ, et al. 2007. Transactivation of miR-34a by p53 broadly influences gene expression and promotes apoptosis. *Mol Cell* **26**: 745–752.
- Choi YJ, Lin C-P, Ho JJ, He X, Okada N, Bu P, Zhong Y, Kim SY, Bennett MJ, Chen C, et al. 2011. miR-34 miRNAs provide a barrier for somatic cell reprogramming. *Nat Cell Biol* **13**: 1353–1360.
- Choudhury AR, Ju Z, Djojotubroto MW, Schienke A, Lechel A, Schaetzlein S, Jiang H, Stepczynska A, Wang C, Buer J, et al. 2007. Cdkn1a deletion improves stem cell function and lifespan of mice with dysfunctional telomeres without accelerating cancer formation. *Nat Genet* **39**: 99–105.
- Concepcion CP, Han Y-C, Mu P, Bonetti C, Yao E, D'Andrea A, Vidigal JA, Maughan WP, Ogradowski P, Ventura A. 2012. Intact p53-dependent responses in miR-34-deficient mice. *PLoS Genet* **8**: e1002797.
- Eischen CM, Lozano G. 2009. p53 and MDM2: Antagonists or partners in crime? *Cancer Cell* **15**: 161–162.
- Feldser DM, Kostova KK, Winslow MM, Taylor SE, Cashman C, Whittaker CA, Sanchez-Rivera FJ, Resnick R, Bronson R, Hemann MT, et al. 2010. Stage-specific sensitivity to p53 restoration during lung cancer progression. *Nature* **468**: 572–575.
- Filipowicz W, Bhattacharyya SN, Sonenberg N. 2008. Mechanisms of post-transcriptional regulation by microRNAs: Are the answers in sight? *Nat Rev Genet* **9**: 102–114.
- Grimson A, Farh KK-H, Johnston WK, Garrett-Engele P, Lim LP, Bartel DP. 2007. MicroRNA targeting specificity in mammals: Determinants beyond seed pairing. *Mol Cell* **27**: 91–105.
- He L, He X, Lim LP, de Stanchina E, Xuan Z, Liang Y, Xue W, Zender L, Magnus J, Ridzon D, et al. 2007. A microRNA component of the p53 tumour suppressor network. *Nature* **447**: 1130–1134.
- Hermeking H. 2007. p53 enters the microRNA world. *Cancer Cell* **12**: 414–418.
- Hermeking H. 2009. The miR-34 family in cancer and apoptosis. *Cell Death Differ* **17**: 193–199.
- Jackson EL, Willis N, Mercer K, Bronson RT, Crowley D, Montoya R, Jacks T, Tuveson DA. 2001. Analysis of lung tumor initiation and progression using conditional expression of oncogenic K-ras. *Genes Dev* **15**: 3243–3248.
- Jackson EL, Olive KP, Tuveson DA, Bronson R, Crowley D, Brown M, Jacks T. 2005. The differential effects of mutant p53 alleles on advanced murine lung cancer. *Cancer Res* **65**: 10280–10288.
- Jain AK, Barton MC. 2012. Unmet expectations: miR-34 plays no role in p53-mediated tumor suppression in vivo. *PLoS Genet* **8**: e1002859.
- Junttila MR, Karnezis AN, Garcia D, Madriles F, Kortlever RM, Rostker F, Swigart LB, Pham DM, Seo Y, Evan GI, et al. 2010. Selective activation of p53-mediated tumour suppression in high-grade tumours. *Nature* **468**: 567–571.
- Kaghad M, Bonnet H, Yang A, Creancier L, Biscan J-C, Valent A, Minty A, Chalou P, Lelias J-M, Dumont X, et al. 1997. Monoallelically expressed gene related to p53 at 1p36, a region frequently deleted in neuroblastoma and other human cancers. *Cell* **90**: 809–819.
- Kasinski AL, Slack FJ. 2012. miRNA-34 prevents cancer initiation and progression in a therapeutically-resistant K-ras and p53-induced mouse model of lung adenocarcinoma. *Cancer Res* **72**: 5576–5587.
- Kim NH, Kim HS, Li X-Y, Lee I, Choi H-S, Kang SE, Cha SY, Ryu JK, Yoon D, Fearon ER, et al. 2011. A p53/miRNA-34 axis regulates Snail1-dependent cancer cell epithelial-mesenchymal transition. *J Cell Biol* **195**: 417–433.
- Kruse J-P, Gu W. 2009. Modes of p53 regulation. *Cell* **137**: 609–622.
- Lal A, Thomas MP, Altschuler G, Navarro F, O'Day E, Li XL, Concepcion C, Han Y-C, Thiery J, Rajani DK, et al. 2011. Capture of microRNA-bound mRNAs identifies the tumor suppressor miR-34a as a regulator of growth factor signaling. *PLoS Genet* **7**: e1002363.
- Lane D, Levine A. 2010. p53 research: The past thirty years and the next thirty years. *Cold Spring Harb Perspect Biol* **2**: a000893.
- Lewis BP, Shih I, Jones-Rhoades MW, Bartel DP. 2003. Prediction of mammalian microRNA targets. *Cell* **115**: 787–798.
- Lewis BP, Burge CB, Bartel DP. 2005. Conserved seed pairing, often flanked by adenosines, indicates that thousands of human genes are microRNA targets. *Cell* **120**: 15–20.
- Lin C-P, Choi YJ, Hicks GG, He L. 2012. The emerging functions of the p53-miRNA network in stem cell biology. *Cell Cycle* **11**: 2063–2072.
- Lodygin D, Tarasov V, Epanchintsev A, Berking C, Knyazeva T, Körner H, Knyazev P, Diebold J, Hermeking H. 2008. Inactivation of miR-34a by aberrant CpG methylation in multiple types of cancer. *Cell Cycle* **7**: 2591–2600.
- Mandke P, Wyatt N, Fraser J, Bates B, Berberich SJ, Markey MP. 2012. MicroRNA-34a modulates MDM4 expression via a target site in the open reading frame. *PLoS ONE* **7**: e42034.
- Marine J-C, Francoz S, Maetens M, Wahl G, Toledo F, Lozano G. 2006. Keeping p53 in check: Essential and synergistic functions of Mdm2 and Mdm4. *Cell Death Differ* **13**: 927–934.
- Markey M, Berberich SJ. 2008. Full-length hdmX transcripts decrease following genotoxic stress. *Oncogene* **27**: 6657–6666.
- Martín-Caballero J, Flores JM, García-Palencia P, Serrano M. 2001. Tumor susceptibility of p21Waf1/Cip1-deficient mice. *Cancer Res* **61**: 6234–6238.
- Michalak EM, Villunger A, Adams JM, Strasser A. 2008. In several cell types tumour suppressor p53 induces apoptosis largely via Puma but Noxa can contribute. *Cell Death Differ* **15**: 1019–1029.
- Migliorini D, Lazzarini Denchi E, Danovi D, Jochemsen A, Capillo M, Gobbi A, Helin K, Pelicci PG, Marine J-C. 2002.

- Mdm4 (Mdmx) regulates p53-induced growth arrest and neuronal cell death during early embryonic mouse development. *Mol Cell Biol* **22**: 5527–5538.
- Miranda KC, Huynh T, Tay Y, Ang Y-S, Tam WL, Thomson AM, Lim B, Rigoutsos I. 2006. A pattern-based method for the identification of microRNA binding sites and their corresponding heteroduplexes. *Cell* **126**: 1203–1217.
- Parant J, Chavez-Reyes A, Little NA, Yan W, Reinke V, Jochemsen AG, Lozano G. 2001. Rescue of embryonic lethality in Mdm4-null mice by loss of Trp53 suggests a nonoverlapping pathway with MDM2 to regulate p53. *Nat Genet* **29**: 92–95.
- Raver-Shapira N, Marciano E, Meiri E, Spector Y, Rosenfeld N, Moskovits N, Bentwich Z, Oren M. 2007. Transcriptional activation of miR-34a contributes to p53-mediated apoptosis. *Mol Cell* **26**: 731–743.
- Riley T, Sontag E, Chen P, Levine A. 2008. Transcriptional control of human p53-regulated genes. *Nat Rev Mol Cell Biol* **9**: 402–412.
- Rodenhuis S, Slebos RJ. 1992. Clinical significance of ras oncogene activation in human lung cancer. *Cancer Res* **52**: 2665s–2669s.
- Slebos RJ, Kibbelaar RE, Dalesio O, Kooistra A, Stam J, Meijer CJ, Wagenaar SS, Vanderschueren RG, van Zandwijk N, Mooi WJ. 1990. K-ras oncogene activation as a prognostic marker in adenocarcinoma of the lung. *N Engl J Med* **323**: 561–565.
- Sun F, Fu H, Liu Q, Tie Y, Zhu J, Xing R, Sun Z, Zheng X. 2008. Downregulation of CCND1 and CDK6 by miR-34a induces cell cycle arrest. *FEBS Lett* **582**: 1564–1568.
- Tanaka N, Toyooka S, Soh J, Kubo T, Yamamoto H, Maki Y, Muraoka T, Shien K, Furukawa M, Ueno T, et al. 2012. Frequent methylation and oncogenic role of microRNA-34b/c in small-cell lung cancer. *Lung Cancer* **76**: 32–38.
- Tarasov V, Jung P, Verdoodt B, Lodygin D, Epanchintsev A, Menssen A, Meister G, Hermeking H. 2007. Differential regulation of microRNAs by p53 revealed by massively parallel sequencing: miR-34a is a p53 target that induces apoptosis and G1-arrest. *Cell Cycle* **6**: 1586–1593.
- Vousden KH, Prives C. 2009. Blinded by the light: The growing complexity of p53. *Cell* **137**: 413–431.
- Wade M, Li Y-C, Wahl GM. 2013. MDM2, MDMX and p53 in oncogenesis and cancer therapy. *Nat Rev Cancer* **13**: 83–96.
- Wang X, Wang J, Jiang X. 2011a. MdmX protein is essential for Mdm2 protein-mediated p53 polyubiquitination. *J Biol Chem* **286**: 23725–23734.
- Wang Z, Chen Z, Gao Y, Li N, Li B, Tan F, Tan X, Lu N, Sun Y, Sun J, et al. 2011b. DNA hypermethylation of microRNA-34b/c has prognostic value for stage I non-small cell lung cancer. *Cancer Biol Ther* **11**: 490–496.
- Wiggins JF, Ruffino L, Kelnar K, Omotola M, Patrawala L, Brown D, Bader AG. 2010. Development of a lung cancer therapeutic based on the tumor suppressor microRNA-34. *Cancer Res* **70**: 5923–5930.
- Winslow MM, Dayton TL, Verhaak RGW, Kim-Kiselak C, Snyder EL, Feldser DM, Hubbard DD, Dupage MJ, Whittaker CA, Hoersch S, et al. 2011. Suppression of lung adenocarcinoma progression by Nkx2-1. *Nature* **473**: 101–104.
- Yamakuchi M, Ferlito M, Lowenstein CJ. 2008. miR-34a repression of SIRT1 regulates apoptosis. *Proc Natl Acad Sci* **105**: 13421–13426.
- Zamore PD, Haley B. 2005. Ribo-gnome: The big world of small RNAs. *Science* **309**: 1519–1524.